Published in final edited form as:
Cell Rep. 2014 April 24; 7(2): 476–487. doi:10.1016/j.celrep.2014.02.048.

E3 Ligase Subunit Fbxo15 and PINK1 Kinase Regulate Cardiolipin Synthase 1 Stability and Mitochondrial Function in Pneumonia

Bill B. Chen[1], **Tiffany A. Coon**[1], **Jennifer R. Glasser**[1], **Chunbin Zou**[1], **Bryon Ellis**[1], **Tuhin Das**[1], **Alison C. McKelvey**[1], **Shristi Rajbhandari**[1], **Travis Lear**[1], **Christelle Kamga**[3], **Sruti Shiva**[3], **Chenjian Li**[6], **Joseph M. Pilewski**[1], **Jason Callio**[4], **Charleen T. Chu**[4], **Anuradha Ray**[1], **Prabir Ray**[1], **Yulia Y. Tyurina**[5], **Valerian E. Kagan**[5], and **Rama K. Mallampalli**[1,2,7,*]

[1]Department of Medicine, Acute Lung Injury Center of Excellence, University of Pittsburgh, Pittsburgh, PA 15213, USA

[2]Department of Cell Biology and Physiology, University of Pittsburgh, Pittsburgh, PA 15213, USA

[3]Vascular Medicine Institute, University of Pittsburgh, Pittsburgh, PA 15213, USA

[4]Department of Pathology, University of Pittsburgh, Pittsburgh, PA 15213, USA

[5]Department of Environmental and Occupational Health, University of Pittsburgh, Pittsburgh, PA 15213, USA

[6]Department of Neurology, Mt. Sinai School of Medicine, New York, NY 10029, USA

[7]Medical Specialty Service Line, Veterans Affairs Pittsburgh Healthcare System, Pittsburgh, PA 15240, USA

SUMMARY

Acute lung injury (ALI) is linked to mitochondrial injury, resulting in impaired cellular oxygen utilization; however, it is unknown how these events are linked on the molecular level. Cardiolipin, a mitochondrial-specific lipid, is generated by cardiolipin synthase (CLS1). Here, we show that *S. aureus* activates a ubiquitin E3 ligase component, Fbxo15, that is sufficient to mediate proteasomal degradation of CLS1 in epithelia, resulting in decreased cardiolipin availability and disrupted mitochondrial function. CLS1 is destabilized by the phosphatase and tensin homolog (PTEN)-induced putative kinase 1 (PINK1), which binds CLS1 to phosphorylate and regulates CLS1 disposal. Like Fbxo15, PINK1 interacts with and regulates levels of CLS1

*Correspondence: mallampallirk@upmc.edu.

SUPPLEMENTAL INFORMATION

Supplemental Information includes seven figures and can be found with this article online at http://dx.doi.org/10.1016/j.celrep.2014.02.048.

AUTHOR CONTRIBUTIONS

R.K.M. was responsible for oversight of the studies; B.B.C. designed the study, performed experiments, analyzed the data, and wrote the manuscript; T.A.C., J.R.G., C.Z., B.E., T.D., C.K., A.C.M., S.R., T.L., and S.S. performed experiments; C.T.C., J.C., and C.L. assisted with animal experiments and provided Pink1 knockout mice; Y.Y.T. performed LC/MS of cardiolipin; C.T.C., A.R., P.R., and V.E.K. assisted with direction of studies and editorial revisions; and R.K.M. revised the manuscript and directed the study.

through a mechanism dependent upon Thr219. *S. aureus* infection upregulates this Fbxo15-PINK1 pathway to impair mitochondrial integrity, and Pink1 knockout mice are less prone to *S. aureus*-induced ALI. Thus, ALI-associated disruption of cellular bioenergetics involves bioeffectors that utilize a phosphodegron to elicit ubiquitin-mediated disposal of a key mitochondrial enzyme.

INTRODUCTION

Acute lung injury (ALI) is a devastating disorder that occurs most often from severe bacterial pneumonia or sepsis and is commonly associated with multiorgan failure. One clinical hallmark of patients with ALI is a profound defect in cellular oxygen consumption and extraction, termed cytopathic dysoxia, the mechanisms of which are not understood at the basic level (Loiacono and Shapiro, 2010; Samsel and Schumacker, 1991; Schumacker and Samsel, 1989; Shoemaker et al., 1993; Singer, 2007). Indeed, significant efforts to enhance tissue oxygenation by increasing oxygen delivery in sepsis have proven ineffective, indicating that a mitochondrial defect contributes to the pathobiology of multiorgan failure. Thus, impaired oxygen utilization may be due to mitochondrial abnormalities and ensuing epithelial apoptosis, both of which have been extensively described in ALI subjects (Brealey et al., 2002; Protti and Singer, 2006; Singer, 2007; Svistunenko et al., 2006). Type II alveolar epithelial cells exhibit on a cellular basis the highest level of pulmonary oxygen utilization and contain ~50% of mitochondria in the lung (Crapo et al., 1978, 1980; Massaro et al., 1975). Thus, an intact mitochondrial apparatus for oxygen utilization at the epithelial cellular level is imperative for these cells to generate the chemical energy needed to maintain pulmonary homeostasis.

Cardiolipin is an integral component of inner mitochondrial membranes and essential for bioenergetics (Choi et al., 2007; McMillin and Dowhan, 2002). Hence, cardiolipin deficiency is lethal, as its impaired production is linked to impaired cell growth and viability (Ostrander et al., 2001). A final step for de novo mitochondrial synthesis of cardiolipin utilizes phosphatidylglycerol and cytidine diphosphate choline-diacylglycerol as substrates in a reaction catalyzed by the enzyme cardiolipin synthase 1 (CLS) (Schlame and Hostetler, 1997). The gene encoding CLS1 was recently cloned from yeast and mammalian sources, and *CLS* knockdown results in impaired cell growth and viability (Chang et al., 1998; Choi et al., 2007; Houtkooper et al., 2006; Jiang et al., 1999; Lu et al., 2006). Interestingly, the CLS transcript (hCLS1) is ubiquitously expressed in tissues but low in whole lung suggestive of its posttranslational regulation (Chen et al., 2006). After initial de novo biosynthesis on the inner membrane of mitochondria, cardiolipin undergoes further remodeling in the mitochondria to incorporate unsaturated fatty acyl groups that confer its structural and biologic activity; this remodeling is catalyzed either by CLS1 itself, tafazzin, or lysocardiolipin acyltransferase (Nie et al., 2010; Xu et al., 2010). CLS1, however, appears to exhibit reacylation activity for lysophosphatidylglycerol rather than lysocardiolipin. The data suggest that, on one hand, cardiolipin has a vitally important structural and physiologic role in mitochondria, as its deficiency leads to cytochrome C release and apoptosis (Choi et al., 2007; McMillin and Dowhan, 2002). However, because of its evolutionarily conserved resemblance to bacterial cardiolipin, the release of mammalian cardiolipin from dying cells

into the extracellular space serves as a highly potent mitochondrial-derived damage-associated molecular pattern (DAMP-CL) that disrupts lung homeostasis (Ray et al., 2010).

Ubiquitination of proteins brands them for degradation either by the proteasome or via the lysosome (Tanaka et al., 2008). The conjugation of ubiquitin to a target protein is orchestrated by a series of enzymatic reactions involving an E1 ubiquitin-activating enzyme, ubiquitin transfer from an E1-activating enzyme to an E2-conjugating enzyme, and last, generation of an iso-peptide bond between the substrate's ε-amino lysine and the carboxyl-terminus of ubiquitin catalyzed by a E3-ubiquitin ligase (Hochstrasser, 2000). Of the many E3 ligases, the SCF superfamily is among the best studied (Tyers and Willems, 1999). The SCF complex has a catalytic core complex consisting of Skp1, Cullin1, and the E2 ubiquitin-conjugating enzyme (Cardozo and Pagano, 2004; Zheng et al., 2002). The SCF complex also contains an adaptor receptor subunit, termed F-box protein, that targets hundreds of substrates through phosphospecific domain interactions (Cenciarelli et al., 1999). F-box proteins have two domains: an NH_2-terminal F-box motif and a carboxyl-terminal leucine-rich repeat motif or tryptophanaspartic acid (WD) repeat motif. The SCF complex uses the F-box motif to bind Skp1, whereas the leucine-rich/WD repeat motif is used for substrate recognition (Ilyin et al., 1999). However, there is a subclass of F-box proteins that lacks a distinct carboxyl-terminal motif, thus named F-box domain only proteins (Fbxos). Of this protein family, the promoter of *FBXO15* was used as reporter to screen pluripotent cells (Okita et al., 2007); the authentication of Fbxo15 as a ubiquitin E3 subunit and its definitive substrate remains unknown, although a recent study suggests it may control levels of p-glycoprotein (Katayama et al., 2013).

Phosphatase and tensin homolog (PTEN)-induced putative kinase 1 (PINK1) is a mitochondrial serine/threonine-protein kinase encoded by the *PINK1* gene (Unoki and Nakamura, 2001). Loss of function mutations in the *PINK1* gene are critically linked to mitochondrial dysfunction and early onset Parkinson's disease (Valente et al., 2004). PINK1 contains an NH_2-terminal mitochondrial-targeting sequence and is predicted to have an important role in mitochondrial function (Mills et al., 2008). PINK1 is able to access mitochondria to regulate degradation of mitochondrial respiratory chain subunits (Vincow et al., 2013). One model suggests that PINK1 accumulates on the outer mitochondrial membrane after cell stress to recruit parkin (a ubiquitin E3 ligase) and regulate mitochondrial removal by mitophagy (Büeler, 2009). Loss of function mutations in parkin are also etiologically linked to familial forms of Parkinson's disease (Bonifati, 2005; Ziviani et al., 2010). To date, parkin, mitochondrial protease HtrA2, mitochondrial chaperone TRAP1, and Akt are the only known molecular targets described for Pink1 (Murata et al., 2011; Plun-Favreau et al., 2007; Pridgeon et al., 2007; Sha et al., 2010). In this study, we have identified the phosphoenzyme CLS1 as a PINK1 target. PINK1 docks at a CLS1 sequence containing Thr^{219} to signal recruitment of Fbxo15 in lung epithelial cells leading to ubiquitination and degradation of CLS1, reduced cardiolipin synthesis, and apoptosis. Moreover, *S. aureus* infection exploits this PINK1-Fbxo15 pathway to impair mitochondrial integrity and produce lung injury. These results provide a unique mechanistic model for studying dysregulated oxygen metabolism and impaired mitochondrial integrity observed in severe pneumonia-associated ALI.

RESULTS

CLS1 Is Essential for Maintaining Cardiolipin Production and Mitochondrial Function

Human lung epithelial (A549) cells were transfected with control plasmid, *CLS1*-small hairpin RNA (shRNA), or a plasmid encoding the *CLS1* gene. To examine de novo cardiolipin synthesis, content of phospholipids was assessed by normal phase liquid chromatography-mass spectrometry (MS) revealing decreased cardiolipin and an increase in the substrate, phosphatidylglycerol after *CLS1*-shRNA (Figure 1A). Further, *CLS1*-shRNA resulted in reduced CLS1 protein levels, whereas *CLS1* plasmid overexpression increased cardiolipin synthesis and CLS1 protein levels (Figure 1B). Cells transfected with control shRNA or *CLS1*-shRNA were also assayed for ATP levels, indicating significantly decreased ATP levels with *CLS1* knockdown, raising the possibility that cell viability is impaired (Figure 1C). Indeed, *CLS1* knockdown induced apoptosis indicated by caspase 3 cleavage (Figure 1D, arrows). To evaluate mitochondrial function, transfected cells were stained with fluorescent DiOC2(3). A low-fluorescent subpopulation was observed using fluorescence-activated cell sorting (FACS) with *CLS1* knockdown, which indicates mitochondrial membrane potential loss (Figure 1E). Interestingly, *CLS1* knockdown also dramatically changed the morphology of mitochondria within the cells from healthy rod-shaped to large dense granules (Figure 1F). Last, JC-1 dye was used to stain mitochondria. JC-1 is a cationic dye that exhibits potential-dependent accumulation in mitochondria, indicated by a fluorescence emission shift from green (~525 nm) to red (~590 nm). *CLS1* knockdown led to mitochondrial depolarization as indicated by a decrease in the red/green fluorescence intensity ratio (Figure 1G).

Fbxo15 Targets CLS1 Protein for Ubiquitination and Degradation, thereby Disrupting Mitochondrial Function

We embarked on an unbiased screen testing proteins that might be involved in CLS1 degradation. Over 27 randomly selected F-box proteins (FBXL, FBXW, and FBXO family members) were ectopically expressed in lung epithelial cells (Figures S1A–S1C) and cells collected and lysates analyzed for expression of F-box proteins and endogenous CLS1. Only expression of Fbxo15 decreased CLS1 levels. To confirm the specificity of Fbxo15 targeting, we performed coimmunoprecipitation (co-IP) experiments. A549 cells were lysed and subjected to CLS1 IP. Of six E3 ligases subunits tested, only Fbxo15 was detected in association with CLS1 (Figure S1D). Further, ectopic Fbxo15 expression significantly decreased half-life ($t_{1/2}$) of CLS1 (Figure 2A). Addition of the proteasomal inhibitor, MG132, to cells led to a significant increase in CLS1 protein half-life, whereas this was not seen with the lysosomal inhibitor, leupeptin (Figure 2B). Thus, endogenous Fbxo15 targets CLS1 for possible ubiquitination. To identify the ubiquitination acceptor site within CLS1, a candidate-mapping approach was used where CLS1 lysine mutants were constructed and synthesized in vitro before testing using ubiquitination assays (Figure S2A). Of several CLS1 point mutants tested, only CLS1-K174R exhibited partial resistance to SCF^{Fbxo15}-directed polyubiquitination (Figure S2B). Finally, the K174R mutant exhibited an extended $t_{1/2}$ compared to wild-type CLS1 (Figure S2C).

To evaluate the biological role of Fbxo15, A549 cells were transfected with an empty plasmid, *Fbxo15*-shRNA, or a plasmid encoding the *Fbxo15* gene prior to assays for cardiolipin synthesis. *Fbxo15* plasmid expression significantly decreased cardiolipin synthesis and CLS1 protein levels, whereas *Fbxo15* knockdown significantly increased cardiolipin production and CLS1 protein levels (Figures 2C and 2D). Hence, Fbxo15 regulates cardiolipin biosynthesis via CLS1 in cells. Next, cells were transfected with *Fbxo15* plasmid to assess mitochondrial morphology. Interestingly, ectopic expression of *Fbxo15* plasmid dramatically changed the morphology of mitochondria within cells from healthy rod-shaped structures to large dense granules (Figure 2E). JC-1 staining revealed that *Fbxo15* plasmid overexpression leads to mitochondrial depolarization as indicated by a decrease in the red/green fluorescence intensity ratio (Figure 2F). These results were also confirmed by FACS analysis and DiOC2(3) staining indicative of a low-fluorescent subpopulation with *Fbxo15* plasmid overexpression, suggestive of mitochondrial membrane potential loss (Figure 2G). *Fbxo15* plasmid overexpression also significantly decreased ATP levels (Figure 2H) coupled with a dose-dependent decrease in immunoreactive CLS1 content (Figure 2I).

PINK Regulates CLS1 Stability

To determine the Fbxo15 docking site within the CLS1, a deletional mapping approach was used where truncated CLS1 mutants were constructed and synthesized in vitro. These synthesized his-tagged mutant CLS1 proteins were then subjected to copurification with Fbxo15 using a cobalt column. All CLS1 constructs were successfully synthesized in vitro, and CLS1 C200 and C150 mutants lacked ability to bind Fbxo15 (Figure S3A). Thus, Fbxo15 docks within the enzyme spanning the region of 200–250 amino acids (aas) within CLS1. Closer examination of this region revealed several potential phosphorylation sites determined by a Net-Phos program (Blom et al., 1999). Site-directed mutagenesis of candidate CLS1 phosphorylation sites was performed, followed by in vitro synthesis and copurification with Fbxo15 using a cobalt column. Of several mutants tested, only a CLS1-T219A lacked ability to bind Fbxo15 (Figure S3B). Thus, T219 within CLS1 serves as a potential molecular recognition site for Fbxo15, consistent with the behavior of SCF members to target phosphodegrons within substrates. Alternatively, this site could serve as a docking or phosphorylation site for a kinase that regulates binding of Fbxo15 to CLS1 indirectly.

To first identify if CLS1 is phosphorylated, A549 cells were lysed and subjected to CLS1 IP and samples probed using phospho-threonine antibodies; the results revealed a band that migrates at the predicted size of CLS1 (Figure 3A). To identify a kinase that phosphorylates CLS1, we performed co-IP experiments. A549 cells were lysed and subjected to CLS1 IP and samples also probed with antibodies against several candidate kinases. Of seven kinases tested, only PINK1 was detected in the CLS1 immunoprecipitates (Figure 3B). In vitro kinase assays using recombinant proteins under various control conditions indicated that PINK1 directly phosphorylates CLS1 (Figure 3C). Additional mapping and pull-down studies indicated that PINK1 kinase also docks within the 200–250 aas region of CLS1 requiring T219 (Figures 3D and 3E). Similar to Fbxo15, knockdown of PINK1 kinase using shRNA increased CLS1 levels, whereas overexpression of *PINK1* plasmid decreased CLS1

levels (Figure S4A). Last, protein half-life studies demonstrated that the T219A CLS1 mutant exhibited a significantly extended $t_{1/2}$ compared to wild-type enzyme and other mutants tested (Figures S4B and S4C). Physiologically, *PINK1* plasmid expression in cells reduced cardiolipin synthesis, ATP levels, and mitochondrial morphologic integrity (Figures 3F–3I), whereas *PINK1* knockdown stimulated cardiolipin synthesis (Figure 3F). Additional studies suggest that CLS1 is degraded within the cytosol rather than in the mitochondria because ectopic *PINK1* or *Fbxo15* plasmid expression was sufficient to reduce immunoreactive CLS1 in soluble fractions of cells and Fbxo15 levels were not detected in mitochondria even after ectopic *Fbxo15* plasmid expression (Figures S5A and S5B). Last, PINK1 depletion using shRNA resulted in reduced levels of polyubiquitinated CLS1 suggesting that the kinase was required for Fbxo15 recruitment to the cardiolipin biosynthetic enzyme (Figure S5C).

S. aureus Activates an Fbxo15/PINK1 Pathway to Impair Mitochondrial Function via CLS1

When *S. aureus* was given to mice (1×10^7 colony-forming units [cfus]/mouse intratracheally [i.t.]) for 3 hr or 6 hr, immunoblotting revealed increased levels of Fbxo15 and PINK1 in whole-lung samples (Figure 4A) and increased association of Fbxo15 to CLS1 that also was bound to PINK1 (Figure 4B). *S. aureus* increased CLS1 phosphorylation (Figure 4B).To evaluate effects of *S. aureus* on murine epithelia, lung type II cells were isolated and cultured with the pathogen. We observed morphologic changes and depolarization in mitochondria by MitoTracker and JC-1 staining (Figure S6A). Similarly, *S. aureus* also increased levels of immunoreactive Fbxo15 and PINK1 and decreased levels of CLS1 in murine type II cells (Figure S6B). *S. aureus* also reduced cardiolipin production and increased release of this mitochondrial-specific DAMP into culture medium (Figures 4C and 4D). JC-1 staining revealed that double knockdown of Fbxo15 and PINK1 protein attenuated mitochondrial depolarization caused by *S. aureus* (Figure 4E). Importantly, oxygen consumption rates in cells were significantly reduced by *PINK1* or *Fbxo15* plasmid overexpression or after *S. aureus* infection (Figure 4F). These results correlated with decreased cardiolipin mass in cells after *PINK1* or *Fbxo15* plasmid overexpression (Figure S6C). Further, expression of *CLS1* plasmid in cells was sufficient to rescue *S. aureus*-induced decreases in ATP production (Figure 4G). Immunoblot analysis from subjects with pneumonia revealed increased PINK1 and Fbxo15 content and decreased CLS1 protein levels in lung tissue (Figure 4H).

Lentiviral Fbxo15 Gene Transfer Induces Acute Lung Injury

To assess the biological significance of Fbxo15, we expressed the F box protein in vivo. We hypothesized that *Fbxo15* gene transfer will decrease CLS1 protein levels, thus reducing mitochondrial function, accentuating pulmonary injury. In mice, lentiviral *Fbxo15* gene transfer decreased CLS1 protein levels (Figure 5A). These effects were associated with increased lung resistance and elastance (lung stiffness), decreased compliance (volume/pressure; Figures 5B–5E), and increased lavage protein concentration and lavage cell counts (Figures 5F and 5G); the F box protein also significantly produced pulmonary edema evidenced by extravasation of Evans blue dye into the lung fluid (Figure 5H). Thus, overexpression of *Fbxo15* mimics many of the physiologic effects seen with *S. aureus* infection in vivo.

Pink1 Knockout Mice Have Reduced Severity of *S. aureus*-Induced Acute Lung Injury

To assess the biological significance of PINK1, mice deficient in the kinase were infected with *S. aureus* (Figure 6). The baseline levels of values of lung mechanics in control mice differed in *Pink1*$^{-/-}$ mice versus mice examined in Figure 5 because of experimental design (strain differences; all mice were infected with *S. aureus*). Nevertheless, *Pink1*$^{-/-}$ mice compared to wild-type littermates had better compliance and reduced lung resistance and elastance (Figures 6A–6D) and decreased lavage protein concentration (Figure 6E). Interestingly, lavage cell counts, bacterial load, and lung histology was not altered between the groups (Figures 6F–6H). Importantly, levels of cardiolipin in lung fluid were significantly reduced in *Pink1*$^{-/-}$ mice versus wild-type mice (Figure 6I), consistent with reduced mitochondrial injury. These results suggest that PINK1 regulates vulnerability to microbial lung injury with limited effects on alveolar inflammation. Moreover, the upregulation of PINK1 by *S. aureus* plays an important role in the pathophysiology of this infection. However, these studies were not designed to assess the long-term effects of PINK1 depletion on other parameters such as survival after *S. aureus* infection. This will be important to fully understand the biological role of this kinase in experimental pneumonia.

DISCUSSION

A profound mitochondrial defect exists during ALI and multiorgan failure, the molecular basis of which is unknown. Here, we show that *S. aureus* infection of epithelia implicated in severe ALI degrades the indispensable mitochondrial enzyme, CLS1, required for cardiolipin biosynthesis. *S. aureus* is a major cause of nosocomial and community-acquired pneumonia but also severe sepsis and endocarditis (Watkins et al., 2012). *S. aureus*-induced pneumonia is common and potentially life-threatening (Osiyemi and Dickinson, 2000; Ragle et al., 2010; Rello et al., 2005; Sidorova and Domnikova, 1999). In recent years, more and more *S. aureus* isolates exhibit methicillin resistance, further presenting a significant challenge in its eradication. Thus, based on its importance in the clinical arena and ability to trigger a mitochondrial apoptotic pathway, this pathogen was selected to assess effects on cardiolipin metabolism (Haslinger et al., 2003). We provide evidence of the molecular regulation of CLS1 protein, demonstrating that a poorly characterized F box protein, Fbxo15, is recruited to CLS1, resulting in its poly-ubiquitination and proteasomal elimination. Indeed, Thr^{219} within CLS1 is a critical molecular recognition or docking site for PINK1; this site also signals Fbxo3 recruitment leading to CLS1 poly-ubiquitination at K^{174}. Fbxo15 alone is sufficient to significantly impair mitochondrial oxygen utilization and lung stability, whereas PINK1 is required to mediate adverse effects of *S. aureus* on pulmonary injury. As a whole, our data suggest that *S. aureus* severely disrupts cardiolipin biosynthesis perhaps through ubiquitination at the CLS1 step, which then leads to extracellular release of preformed cardiolipin (Figures 4D and 7). We have previously shown that extracellular cardiolipin potently disrupts lung homeostasis and recapitulates many features of pneumonia (Ray et al., 2010). Hence, our data suggest that, as one mechanism, severe bacterial infection triggers phosphorylation-dependent ubiquitination of a key substrate (CLS1) as a means to release a mitochondrial-derived DAMP to elicit pulmonary dyshomeostasis.

Aside from few initial studies (Chen et al., 2006; Su and Dowhan, 2006), the structure-function and posttranslational control of CLS1 is largely unknown. There appears to be tight coordination between translation and transcription of CLS in yeast (Su and Dowhan, 2006). Further, thyroxine has been shown to increase hepatic enzyme activity (Hostetler, 1991) and lipopolysaccharide decreases CLS mRNA levels in the liver (Lu et al., 2011). CLS1 normally resides within the inner membrane of mitochondria (Chen et al., 2006), where it could potentially colocalize with a pool of PINK1 (Meissner et al., 2011). However, due to lack of a canonical mitochondrial targeting signal, it is unlikely that Fbxo15 traffics inside the mitochondria. More likely, our data suggest that Fbxo15 mediates ubiquitinylation and degradation of CLS1 within the endoplasmic reticulum (ER) after its biosynthesis, perhaps as a feedback regulatory mechanism. Indeed, fractionation studies suggest that mitochondria are devoid of significant concentrations of Fbxo15 under native conditions or after ectopic expression of Fbxo15 (Figure S5). Yet F box protein or *PINK1* plasmid expression reduces CLS1 immunoreactive levels in the cytosol and in the mitochondria (Figure S5). These results suggest that, once Fbxo15-mediated CLS1 depletion occurs in the ER, this limits enzyme targeted to mitochondria. This model is supported by recent evidence of crosstalk and physical contact sites between mitochondria and the ER that facilitate phospholipid synthesis (Friedman et al., 2011). We cannot exclude a mechanism whereby PINK1-induced CLS1 phosphorylation triggers a structural or conformational change in CLS1 to stimulate its release from the inner membrane to the outer membrane of mitochondria, making it accessible for Fbxo15 targeting. In this way, CLS1 ubiquitination by Fbxo15 would mimic interaction on the outer mitochondrial membrane between mitofusin with the E3 ligase component, parkin (Ziviani et al., 2010).

Cardiolipin is synthesized via the biosynthetic pathway involving CLS1 but then is remodeled on the outer mitochondrial membrane by additional enzymes. Our data suggest a central role for CLS1 in preserving mitochondrial integrity in human lung epithelia, as knockdown of *CLS1* reduces cardiolipin production, decreases cardiolipin mass, and leads to loss of mitochondrial functionality. Even though overexpression of *CLS1* increases cardiolipin production and total cardiolipin levels in cells (Chen et al., 2006), other related enzymes involved in its remodeling, including lysocardiolipin acyltransferase or tafazzin, might also be critical targets for E3 ligases. However, decreased total cardiolipin mass (Figure S6C) in cells correlates with reduced CLS1 protein and Fbxo15 and PINK1 appear to selectively target CLS1 (data not shown), underscoring the physiological importance of the CL biosynthetic pathway in lung epithelia. The connection between the de novo and remodeling pathway for cardiolipin synthesis and molecular regulation of related enzymes requires further investigation.

Loss of function mutations in PINK1 gene are major causes of mitochondrial dysfunction resulting in some forms of Parkinson's disease (Valente et al., 2004). However, here, overexpression of *PINK1* caused mitochondrial depolarization and significantly reduced cellular oxygen consumption via triggering CLS1 degradation (Figure 4F). The ability of PINK1 to mediate turnover of mitochondrial proteins is not unusual given its role in modulating stability of membrane-bound respiratory chain subunits (Vincow et al., 2013). Further, compared to wild-type littermates, *Pink1*$^{3}/^{3}$ mice were less prone to *S. aureus*-

induced injury, as reflected by better lung mechanics and lower protein concentrations, with no effect on inflammatory cell recruitment in lung fluid. These results suggest that *S. aureus* primarily impairs lung biophysical properties (e.g., reduces surfactant activity) in a PINK1-dependent manner. Interestingly, *S. aureus* also exploits PINK1 to phosphorylate other substrates such as AKT and Parkin, as PINK1 knockdown effectively prevents *S. aureus*-induced phosphorylation of AKT and Parkin (Figure S7).

Importantly, cardiolipin levels were reduced in lung fluid of infected *Pink1*$^{-/-}$ mice versus control mice, indicating that PINK1 depletion attenuates the ability of *S. aureus* to trigger release of cardiolipin-DAMP. Hence, PINK1 depletion may be protective to microbial virulence under some conditions and its varying roles might simply relate to differences in the cellular systems studied. This is similar to the effects of PINK1 on mitochondrial fission, in which apparently opposite effects are observed in cultured mammalian neurons compared to *Drosophila* muscle and spermatids (Dagda et al., 2009; Deng et al., 2008; Lutz et al., 2009). In this regard, a key feature of lung epithelia is that they are highly enriched with mitochondria, suggesting a need in these cells for mechanisms to provide feedback inhibition to ensure tight homeostatic control of levels of proteins within the mitochondrial apparatus. Hence, PINK1 and Fbxo15 might represent a constitutive mechanism to limit an overabundance of CLS1, and yet this pathway could to be exploited in settings of pulmonary inflammation during severe infection with highly virulent bacterial pathogens.

EXPERIMENTAL PROCEDURES

Cell Culture and Transfection

A549 cells were cultured in F12/K medium (Gibco) supplemented with 10% fetal bovine serum. For half-life studies, cells were treated with cycloheximide (40 μg/ml) at different time points in blank medium. Cells lysates were prepared by brief sonication in 150 mM NaCl, 50 mM Tris, 1.0 mM EDTA, 2 mM dithiothreitol, 0.025% sodium azide, and 1 mM phenylmethylsulfonyl fluoride (buffer A) at 4°C. All plasmids were delivered into cells using Fugene 6HD. All plasmid constructs were generated using PCR-based strategies using appropriate primers; point mutants were generated using a site-directed mutagenesis kit (Chen and Mallampalli, 2009).

S. aureus Infection

A549 or murine type II cells were cultured in 6-well dishes at 0.5 million cells/plate for 24 hr before infection. *S. aureus* (A) was purchased from American Type Culture Collection (ATCC). Inoculums were freshly prepared prior to experiments using frozen stocks of *S. aureus* (ATCC strain 29213, frozen at midlog phase; optical density 625 = 0.8). *S. aureus* was maintained in tryptic soy broth minimal agar. Cultures were plated and grown overnight from frozen stock. Overnight plate cultures were then inoculated in tryptic soy broth and grown by rotary shaking at 37°C to log phase. Cells were then infected with *S. aureus* at multiplicity of infection (moi) = 10, 50, or 100 for 1, 2, or 16 hr.

Coimmunoprecipitation

Five hundred micrograms of total protein from cell lysates was precleared with 20 μl of protein A/G beads for 1 hr at 4°C. Five micrograms of primary antibody was added for 18 hr incubation at 4°C. Forty microliters of protein A/G beads were added for an additional 6 hr of incubation. Beads were slowly centrifuged and washed five times using 50 mM HEPES, 150 mM NaCl, 0.5 mM EGTA, 50 mM NaF, 10 mM Na_3VO_4, 1 mM phenylmethylsulfonyl fluoride, 20 μM leupeptin, and 1% (v/v) Triton X-100 (radio-immunoprecipitation assay) buffer, as described (Mallampalli et al., 2000). The beads were heated at 100°C for 5 min with 80 μl of protein sample buffer prior to SDS-PAGE and immunoblotting. CLS1 (Novus; Santa Cruz Biotechnology), Fbxo15 (Novus; GeneTex), and PINK1 primary antibodies (Abcam) were used at 1:500 to 1:1,000 dilution in immunoblotting.

Mass Spectrometry and Liquid Chromatography

Cellular lipids were extracted using the method of Folch (Folch et al., 1957). Cardiolipin resolved using high-performance thin-layer chromatography and analyzed by liquid chromatography (LC)/MS using a Prominence high-performance liquid chromatography system (Shimadzu) with a reverse phase C_8 column (Luna; 5 micron; 4.6 mm × 15 cm; Phenomenex). An isocratic solvent system (2-propanol: water: triethylamine: acetic acid; 450:50:2.5:2.5; v/v/v/v) was used at a flow rate of 0.4 ml/min. Spectra were analyzed on Q-TOF Premier mass spectrometer (Waters). Parameters of MS and details were described previously (Tyurina et al., 2011).

Microscopy and Immunostaining

All the microscopy work was performed using a Nikon A1 confocal microscope using a 60× oil objective. The microscope was equipped with Ti Perfect Focus system and Tokai Hit live cell chamber providing a humidified atmosphere at 37°C with 5% CO_2. Transfected cells (2×10^5) were plated at 70% confluence on 35 mm MatTek glass bottom culture dishes before being labeled with either MitoTracker Red (1:5,000) or JC-1 (1:100) for 20 min. Image analysis was by Nikon NIS-element and ImageJ software.

Mitochondrial Lipids and Bioenergetics

A549 cells were transfected with control shRNA, *Fbxo15*-shRNA or *PINK1* shRNA, or plasmids encoding either *Fbxo15* or *PINK1* for 48 hr. Cells were labeled with [^{3}H]-palmitic acid for additional 24 hr for determination of cardiolipin synthesis. Cells and medium were collected and lipids extracted and separated by thin-layer chromatography (TLC) (Ray et al., 2010). Individual phospholipids on the TLC plates were quantified using a plate reader. ATP was assayed using a CellTiter-Glo Assay kit (Promega). Oxygen consumption in cells was assayed using an XF Analyzer (Seahorse Biosciences).

Animal Studies

Male C57LB/6 mice (purchased from Jackson Laboratories) were acclimated at the University of Pittsburgh Animal Care Facility and maintained according to all federal and institutional animal care guidelines and under a University of Pittsburgh Institutional Animal Care and Use Committee-approved protocol. *Pink1* knockout mice are maintained as a

heterozygous line on a C57/129 background and crossed to generate *Pink*1$^{+/+}$ and *Pink1*$^{-/-}$ littermates (Dagda et al., 2011). Mice were deeply anesthetized with ketamine (80–100 mg/kg of body weight, intraperitoneally [i.p.]) and xylazine (10 mg/kg, i.p.), and then the larynx was well visualized under a fiber optic light source before endotracheal intubation with a 3/400 24-gauge plastic catheter. Replication-deficient lentivirus (Lenti) alone or Lenti-Fbxo15 (10^8 plaque-forming units in 50 μl of PBS) was instilled i.t. on day 1, after which animals were allowed to recover for 96 hr before FlexiVent studies (Chen et al., 2011).

Human Samples

Human lung samples were obtained from the University of Pittsburgh Health Sciences Tissue Bank. The control subjects' ages ranged from 50 to 62, whereas in pneumonia subjects, the ages ranged from 12 to 60. All subjects were Caucasian and female, except one male in the control group. The study was approved both by the University of Pittsburgh Tissue Utilization Committee and University of Pittsburgh Institutional Review Board.

Statistical Analysis

Statistical comparisons were performed with the Prism program, version 4.03 (GraphPad Software) using an ANOVA 1 or an unpaired 2 t test with $p < 0.05$ indicative of significance.

Supplementary Material

Refer to Web version on PubMed Central for supplementary material.

Acknowledgments

This material is based upon work supported, in part, by the US Department of Veterans Affairs, Veterans Health Administration, Office of Research and Development, Biomedical Laboratory Research and Development. This work was supported by a Merit Review Award from the US Department of Veterans Affairs and National Institutes of Health R01 grants HL096376, HL097376, HL098174, HL081784, and P01HL114453 (to R.K.M.); HL116472 (to B.B.C.); NS065789 (to C.T.C.); and 12SDG12040330 (to C.Z.). The contents presented do not represent the views of the Department of Veterans Affairs or the United States Government.

References

Blom N, Gammeltoft S, Brunak S. Sequence and structure-based prediction of eukaryotic protein phosphorylation sites. J Mol Biol. 1999; 294:1351–1362. [PubMed: 10600390]

Bonifati V. Genetics of Parkinson's disease. Minerva Med. 2005; 96:175–186. [PubMed: 16175160]

Brealey D, Brand M, Hargreaves I, Heales S, Land J, Smolenski R, Davies NA, Cooper CE, Singer M. Association between mitochondrial dysfunction and severity and outcome of septic shock. Lancet. 2002; 360:219–223. [PubMed: 12133657]

Büeler H. Impaired mitochondrial dynamics and function in the pathogenesis of Parkinson's disease. Exp Neurol. 2009; 218:235–246. [PubMed: 19303005]

Cardozo T, Pagano M. The SCF ubiquitin ligase: insights into a molecular machine. Nat Rev Mol Cell Biol. 2004; 5:739–751. [PubMed: 15340381]

Cenciarelli C, Chiaur DS, Guardavaccaro D, Parks W, Vidal M, Pagano M. Identification of a family of human F-box proteins. Curr Biol. 1999; 9:1177–1179. [PubMed: 10531035]

Chang SC, Heacock PN, Mileykovskaya E, Voelker DR, Dowhan W. Isolation and characterization of the gene (CLS1) encoding cardiolipin synthase in Saccharomyces cerevisiae. J Biol Chem. 1998; 273:14933–14941. [PubMed: 9614098]

Chen BB, Mallampalli RK. Masking of a nuclear signal motif by monoubiquitination leads to mislocalization and degradation of the regulatory enzyme cytidylyltransferase. Mol Cell Biol. 2009; 29:3062–3075. [PubMed: 19332566]

Chen D, Zhang XY, Shi Y. Identification and functional characterization of hCLS1, a human cardiolipin synthase localized in mitochondria. Biochem J. 2006; 398:169–176. [PubMed: 16716149]

Chen BB, Coon TA, Glasser JR, Mallampalli RK. Calmodulin antagonizes a calcium-activated SCF ubiquitin E3 ligase subunit, FBXL2, to regulate surfactant homeostasis. Mol Cell Biol. 2011; 31:1905–1920. [PubMed: 21343341]

Choi SY, Gonzalvez F, Jenkins GM, Slomianny C, Chretien D, Arnoult D, Petit PX, Frohman MA. Cardiolipin deficiency releases cytochrome c from the inner mitochondrial membrane and accelerates stimuli-elicited apoptosis. Cell Death Differ. 2007; 14:597–606. [PubMed: 16888643]

Crapo JD, Peters-Golden M, Marsh-Salin J, Shelburne JS. Pathologic changes in the lungs of oxygen-adapted rats: a morphometric analysis. Lab Invest. 1978; 39:640–653. [PubMed: 739764]

Crapo JD, Barry BE, Foscue HA, Shelburne J. Structural and biochemical changes in rat lungs occurring during exposures to lethal and adaptive doses of oxygen. Am Rev Respir Dis. 1980; 122:123–143. [PubMed: 7406333]

Dagda RK, Cherra SJ 3rd, Kulich SM, Tandon A, Park D, Chu CT. Loss of PINK1 function promotes mitophagy through effects on oxidative stress and mitochondrial fission. J Biol Chem. 2009; 284:13843–13855. [PubMed: 19279012]

Dagda RK, Gusdon AM, Pien I, Strack S, Green S, Li C, Van Houten B, Cherra SJ 3rd, Chu CT. Mitochondrially localized PKA reverses mitochondrial pathology and dysfunction in a cellular model of Parkinson's disease. Cell Death Differ. 2011; 18:1914–1923. [PubMed: 21637291]

Deng H, Dodson MW, Huang H, Guo M. The Parkinson's disease genes pink1 and parkin promote mitochondrial fission and/or inhibit fusion in Drosophila. Proc Natl Acad Sci USA. 2008; 105:14503–14508. [PubMed: 18799731]

Folch J, Lees M, Sloane Stanley GH. A simple method for the isolation and purification of total lipides from animal tissues. J Biol Chem. 1957; 226:497–509. [PubMed: 13428781]

Friedman JR, Lackner LL, West M, DiBenedetto JR, Nunnari J, Voeltz GK. ER tubules mark sites of mitochondrial division. Science. 2011; 334:358–362. [PubMed: 21885730]

Haslinger B, Strangfeld K, Peters G, Schulze-Osthoff K, Sinha B. Staphylococcus aureus alpha-toxin induces apoptosis in peripheral blood mononuclear cells: role of endogenous tumour necrosis factor-alpha and the mitochondrial death pathway. Cell Microbiol. 2003; 5:729–741. [PubMed: 12969378]

Hochstrasser M. Biochemistry. All in the ubiquitin family. Science. 2000; 289:563–564. [PubMed: 10939967]

Hostetler KY. Effect of thyroxine on the activity of mitochondrial cardiolipin synthase in rat liver. Biochim Biophys Acta. 1991; 1086:139–140. [PubMed: 1659453]

Houtkooper RH, Akbari H, van Lenthe H, Kulik W, Wanders RJ, Frentzen M, Vaz FM. Identification and characterization of human cardiolipin synthase. FEBS Lett. 2006; 580:3059–3064. [PubMed: 16678169]

Ilyin GP, Rialland M, Glaise D, Guguen-Guillouzo C. Identification of a novel Skp2-like mammalian protein containing F-box and leucine-rich repeats. FEBS Lett. 1999; 459:75–79. [PubMed: 10508920]

Jiang F, Gu Z, Granger JM, Greenberg ML. Cardiolipin synthase expression is essential for growth at elevated temperature and is regulated by factors affecting mitochondrial development. Mol Microbiol. 1999; 31:373–379. [PubMed: 9987137]

Katayama K, Noguchi K, Sugimoto Y. FBXO15 regulates P-glycoprotein/ABCB1 expression through the ubiquitin—proteasome pathway in cancer cells. Cancer Sci. 2013; 104:694–702. [PubMed: 23465077]

Loiacono LA, Shapiro DS. Detection of hypoxia at the cellular level. Crit Care Clin. 2010; 26:409–421. [PubMed: 20381729]

Lu B, Xu FY, Jiang YJ, Choy PC, Hatch GM, Grunfeld C, Fein-gold KR. Cloning and characterization of a cDNA encoding human cardiolipin synthase (hCLS1). J Lipid Res. 2006; 47:1140–1145. [PubMed: 16547353]

Lu B, Xu FY, Taylor WA, Feingold KR, Hatch GM. Cardiolipin synthase-1 mRNA expression does not correlate with endogenous cardiolipin synthase enzyme activity in vitro and in vivo in mammalian lipopolysaccharide models of inflammation. Inflammation. 2011; 34:247–254. [PubMed: 20652826]

Lutz AK, Exner N, Fett ME, Schlehe JS, Kloos K, Lämmermann K, Brunner B, Kurz-Drexler A, Vogel F, Reichert AS, et al. Loss of parkin or PINK1 function increases Drp1-dependent mitochondrial fragmentation. J Biol Chem. 2009; 284:22938–22951. [PubMed: 19546216]

Mallampalli RK, Ryan AJ, Salome RG, Jackowski S. Tumor necrosis factor-alpha inhibits expression of CTP:phosphocholine cytidylyltransferase. J Biol Chem. 2000; 275:9699–9708. [PubMed: 10734122]

Massaro GD, Gail DB, Massaro D. Lung oxygen consumption and mitochondria of alveolar epithelial and endothelial cells. J Appl Physiol. 1975; 38:588–592. [PubMed: 1141087]

McMillin JB, Dowhan W. Cardiolipin and apoptosis. Biochim Biophys Acta. 2002; 1585:97–107. [PubMed: 12531542]

Meissner C, Lorenz H, Weihofen A, Selkoe DJ, Lemberg MK. The mitochondrial intramembrane protease PARL cleaves human Pink1 to regulate Pink1 trafficking. J Neurochem. 2011; 117:856–867. [PubMed: 21426348]

Mills RD, Sim CH, Mok SS, Mulhern TD, Culvenor JG, Cheng HC. Biochemical aspects of the neuroprotective mechanism of PTEN-induced kinase-1 (PINK1). J Neurochem. 2008; 105:18–33. [PubMed: 18221368]

Murata H, Sakaguchi M, Jin Y, Sakaguchi Y, Futami J, Yamada H, Kataoka K, Huh NH. A new cytosolic pathway from a Parkinson disease-associated kinase, BRPK/PINK1: activation of AKT via mTORC2. J Biol Chem. 2011; 286:7182–7189. [PubMed: 21177249]

Nie J, Hao X, Chen D, Han X, Chang Z, Shi Y. A novel function of the human CLS1 in phosphatidylglycerol synthesis and remodeling. Biochim Biophys Acta. 2010; 1801:438–445. [PubMed: 20025994]

Okita K, Ichisaka T, Yamanaka S. Generation of germline-competent induced pluripotent stem cells. Nature. 2007; 448:313–317. [PubMed: 17554338]

Osiyemi O, Dickinson G. Gram-Positive Pneumonia. Curr Infect Dis Rep. 2000; 2:207–214. [PubMed: 11095858]

Ostrander DB, Sparagna GC, Amoscato AA, McMillin JB, Dowhan W. Decreased cardiolipin synthesis corresponds with cytochrome c release in palmitate-induced cardiomyocyte apoptosis. J Biol Chem. 2001; 276:38061–38067. [PubMed: 11500520]

Plun-Favreau H, Klupsch K, Moisoi N, Gandhi S, Kjaer S, Frith D, Harvey K, Deas E, Harvey RJ, McDonald N, et al. The mitochondrial protease HtrA2 is regulated by Parkinson's disease-associated kinase PINK1. Nat Cell Biol. 2007; 9:1243–1252. [PubMed: 17906618]

Pridgeon JW, Olzmann JA, Chin LS, Li L. PINK1 protects against oxidative stress by phosphorylating mitochondrial chaperone TRAP1. PLoS Biol. 2007; 5:e172. [PubMed: 17579517]

Protti A, Singer M. Bench-to-bedside review: potential strategies to protect or reverse mitochondrial dysfunction in sepsis-induced organ failure. Crit Care. 2006; 10:228. [PubMed: 16953900]

Ragle BE, Karginov VA, Bubeck Wardenburg J. Prevention and treatment of Staphylococcus aureus pneumonia with a beta-cyclodextrin derivative. Antimicrob Agents Chemother. 2010; 54:298–304. [PubMed: 19805564]

Ray NB, Durairaj L, Chen BB, McVerry BJ, Ryan AJ, Donahoe M, Waltenbaugh AK, O'Donnell CP, Henderson FC, Etscheidt CA, et al. Dynamic regulation of cardiolipin by the lipid pump Atp8b1 determines the severity of lung injury in experimental pneumonia. Nat Med. 2010; 16:1120–1127. [PubMed: 20852622]

Rello J, Sole-Violan J, Sa-Borges M, Garnacho-Montero J, Muñoz E, Sirgo G, Olona M, Diaz E. Pneumonia caused by oxacillin-resistant Staphylococcus aureus treated with glycopeptides. Crit Care Med. 2005; 33:1983–1987. [PubMed: 16148469]

Samsel RW, Schumacker PT. Oxygen delivery to tissues. Eur Respir J. 1991; 4:1258–1267. [PubMed: 1804674]

Schlame M, Hostetler KY. Cardiolipin synthase from mammalian mitochondria. Biochim Biophys Acta. 1997; 1348:207–213. [PubMed: 9370335]

Schumacker PT, Samsel RW. Oxygen delivery and uptake by peripheral tissues: physiology and pathophysiology. Crit Care Clin. 1989; 5:255–269. [PubMed: 2650817]

Sha D, Chin LS, Li L. Phosphorylation of parkin by Parkinson disease-linked kinase PINK1 activates parkin E3 ligase function and NF-kappaB signaling. Hum Mol Genet. 2010; 19:352–363. [PubMed: 19880420]

Shoemaker WC, Appel PL, Kram HB, Bishop MH, Abraham E. Temporal hemodynamic and oxygen transport patterns in medical patients. Septic shock. Chest. 1993; 104:1529–1536. [PubMed: 8222819]

Sidorova LD, Domnikova NP. Prognosis of nosocomial pneumonia outcome. Ter Arkh. 1999; 71:37–40. [PubMed: 10647199]

Singer M. Mitochondrial function in sepsis: acute phase versus multiple organ failure. Crit Care Med. 2007; 35:S441–S448. [PubMed: 17713391]

Su X, Dowhan W. Regulation of cardiolipin synthase levels in Saccharomyces cerevisiae. Yeast. 2006; 23:279–291. [PubMed: 16544270]

Svistunenko DA, Davies N, Brealey D, Singer M, Cooper CE. Mitochondrial dysfunction in patients with severe sepsis: an EPR interrogation of individual respiratory chain components. Biochim Biophys Acta. 2006; 1757:262–272. [PubMed: 16626626]

Tanaka Y, Tanaka N, Saeki Y, Tanaka K, Murakami M, Hirano T, Ishii N, Sugamura K. c-Cbl-dependent monoubiquitination and lysosomal degradation of gp130. Mol Cell Biol. 2008; 28:4805–4818. [PubMed: 18519587]

Tyers M, Willems AR. One ring to rule a superfamily of E3 ubiquitin ligases. Science. 1999; 284:601, 603–604. [PubMed: 10328744]

Tyurina YY, Kisin ER, Murray A, Tyurin VA, Kapralova VI, Sparvero LJ, Amoscato AA, Samhan-Arias AK, Swedin L, Lahesmaa R, et al. Global phospholipidomics analysis reveals selective pulmonary peroxidation profiles upon inhalation of single-walled carbon nanotubes. ACS Nano. 2011; 5:7342–7353. [PubMed: 21800898]

Unoki M, Nakamura Y. Growth-suppressive effects of BPOZ and EGR2, two genes involved in the PTEN signaling pathway. Oncogene. 2001; 20:4457–4465. [PubMed: 11494141]

Valente EM, Salvi S, Ialongo T, Marongiu R, Elia AE, Caputo V, Romito L, Albanese A, Dallapiccola B, Bentivoglio AR. PINK1 mutations are associated with sporadic early-onset parkinsonism. Ann Neurol. 2004; 56:336–341. [PubMed: 15349860]

Vincow ES, Merrihew G, Thomas RE, Shulman NJ, Beyer RP, MacCoss MJ, Pallanck LJ. The PINK1-Parkin pathway promotes both mitophagy and selective respiratory chain turnover in vivo. Proc Natl Acad Sci USA. 2013; 110:6400–6405. [PubMed: 23509287]

Watkins RR, David MZ, Salata RA. Current concepts on the virulence mechanisms of meticillin-resistant Staphylococcus aureus. J Med Microbiol. 2012; 61:1179–1193. [PubMed: 22745137]

Xu FY, McBride H, Acehan D, Vaz FM, Houtkooper RH, Lee RM, Mowat MA, Hatch GM. The dynamics of cardiolipin synthesis post-mitochondrial fusion. Biochim Biophys Acta. 2010; 1798:1577–1585. [PubMed: 20434430]

Zheng N, Schulman BA, Song L, Miller JJ, Jeffrey PD, Wang P, Chu C, Koepp DM, Elledge SJ, Pagano M, et al. Structure of the Cul1-Rbx1-Skp1-F boxSkp2 SCF ubiquitin ligase complex. Nature. 2002; 416:703–709. [PubMed: 11961546]

Ziviani E, Tao RN, Whitworth AJ. Drosophila parkin requires PINK1 for mitochondrial translocation and ubiquitinates mitofusin. Proc Natl Acad Sci USA. 2010; 107:5018–5023. [PubMed: 20194754]

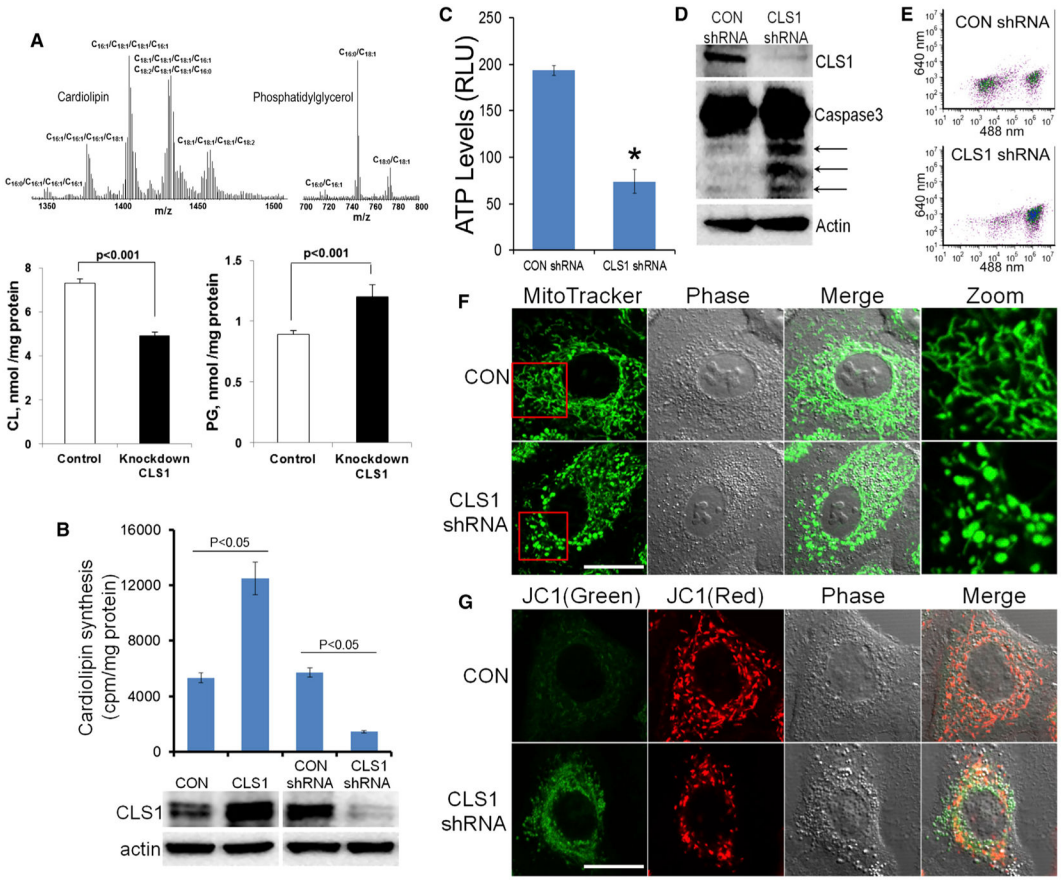

Figure 1. CLS1 Is Essential for Preserving Mitochondrial Function and Structure

(A) A549 cells were transfected with control plasmid shRNA, *CLS1*-shRNA, or a plasmid encoding *CLS1* for 48 hr. Shown is LC-MS assessment of cardiolipin and phosphatidylglycerol in A549 cells. Typical negative-mass spectra of cardiolipin (left, CL) and phosphatidylglycerol (right, PG) obtained from A549 cells above. Below is shown content of CL and PG in control A549 cells and cells after knockdown of *CLS1*. Content of phospholipids was assessed by normal-phase LC-MS. The results are presented as mean ± SD; n = 3. Statistical analyses were performed by Student's t test. The statistical significance of differences was set at $p < 0.05$.

(B) A549 cells were transfected with control (CON) plasmid, *CLS1*-shRNA, or a plasmid encoding *CLS1* for 48 hr. Cells were also labeled with [^{3}H]-palmitic acid for an additional 24 hr after plasmid transfection. Cells were collected and lipids extracted and separated by thin-layer chromatography (TLC). The lipids were quantified using a plate reader, and the radioactivity of the spots was counted and graphed (results are presented as mean ± SE; n = 3 experiments; *$p < 0.05$ versus CON). Below: cell lysates were assayed for levels of immunoreactive hCLS1 and actin proteins.

(C) ATP levels were assayed in cells using the Cell-Glo ATP assay following the manufacturer's protocol (results are presented as mean ± SE; n = 5 experiments; *$p < 0.01$ versus CON). RLU, relative light units.

(D) A549 cells were transfected with control shRNA or *CLS1*-shRNA for 48 hr, and cells were collected and assayed for caspase 3 immunoblotting, indicating cleavage products (arrows).

(E) A549 cells were transfected with control shRNA or *CLS1*-shRNA for 48 hr, and cells were stained with fluorescent DiOC2(3) dye followed by FACS analysis.

(F) Cells were stained with MitoTracker Green to visualize mitochondria; cells were then analyzed by confocal microscopy.

(G) A549 cells were stained with JC-1 dye; the fluorescence emission at channel green (~525 nm) and red (~590 nm) was recorded. Scale bar represents 10 μM.

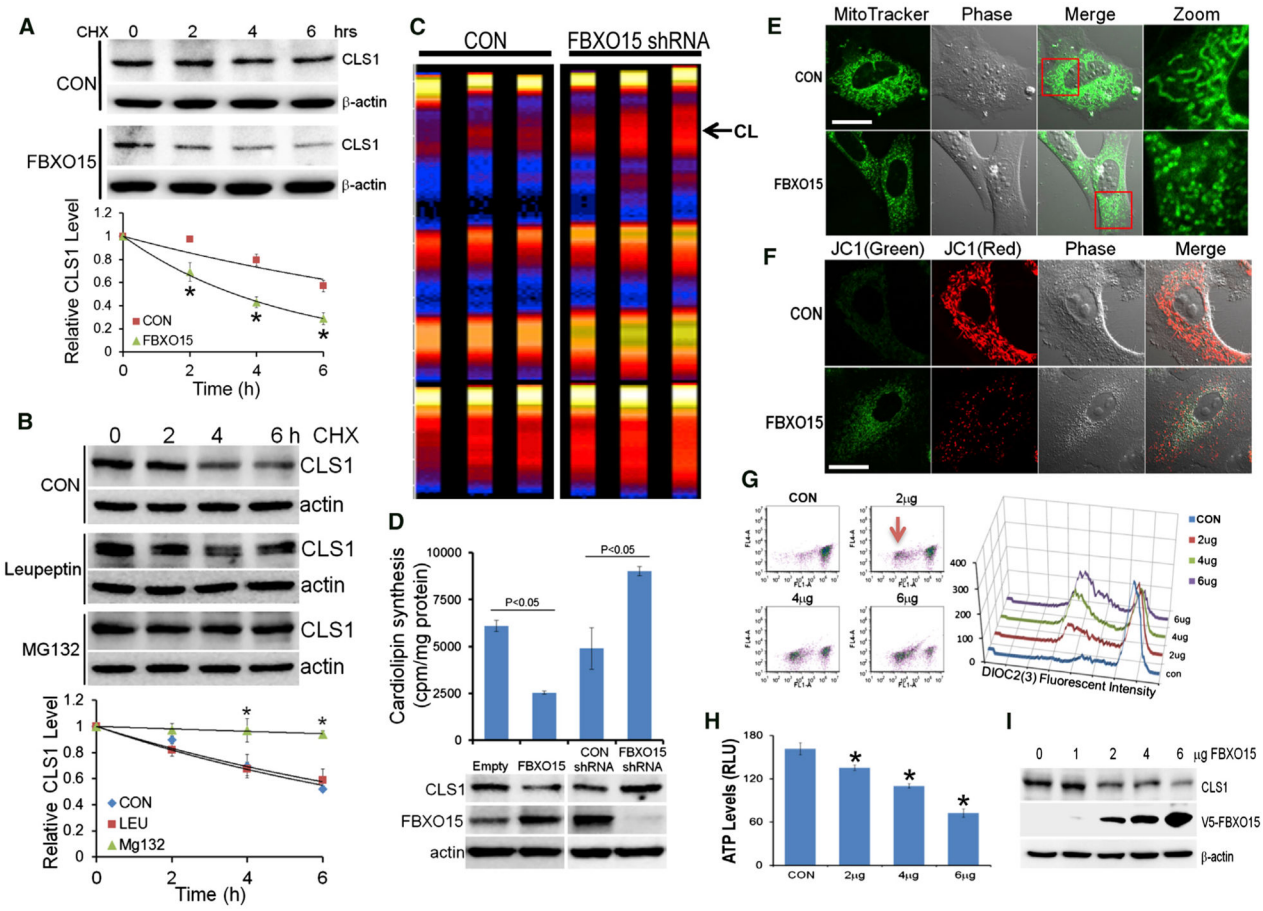

Figure 2. Fbxo15 Targets CLS1 Protein for Ubiquitination and Degradation to Disrupt Mitochondrial Function

(A) CLS1 protein half-life determination with *Fbxo15* overexpression or without (CON; n = 3 experiments; *p < 0.01 versus CON).

(B) CLS1 protein half-life determination using cyclohexamide (CHX) without or with MG132 or leupeptin (LEU) (n = 3 experiments; *p < 0.01 versus CON).

(C and D) A549 cells were transfected with control shRNA, *Fbxo15*-shRNA, or a plasmid encoding *Fbxo15* for 48 hr. Cells were labeled with [^{3}H]-palmitic acid for additional 24 hr. Cells were collected and lipids extracted and separated by TLC. The TLC plate was quantified using a plate reader, the radioactivity of spots counted and graphed in (D), and samples processed for immunoblotting below (n = 3 experiments; *p < 0.05 versus CON or empty plasmid).

(E and F) A549 cells were transfected with *Fbxo15* before staining with MitoTracker Green (E) or JC-1 (F).

(G) A549 cells were transfected with increasing amounts of *Fbxo15* plasmid before staining with DIOC2(3); cells were then analyzed by FACS.

(H) ATP levels were assayed in *Fbxo15*-transfected A549 cells using a Cell-Glo ATP assay (n = 5 experiments; *p < 0.01 versus CON).

(I) Cells were transfected with increasing amounts of *Fbxo15* plasmid. Cells were collected and cell lysates analyzed for V5, CLS1, and β-actin immunoblotting (n = 2). Scale bar represents 10 μM.

Results in (A), (B), (D), and (H) are presented as mean ± SE.

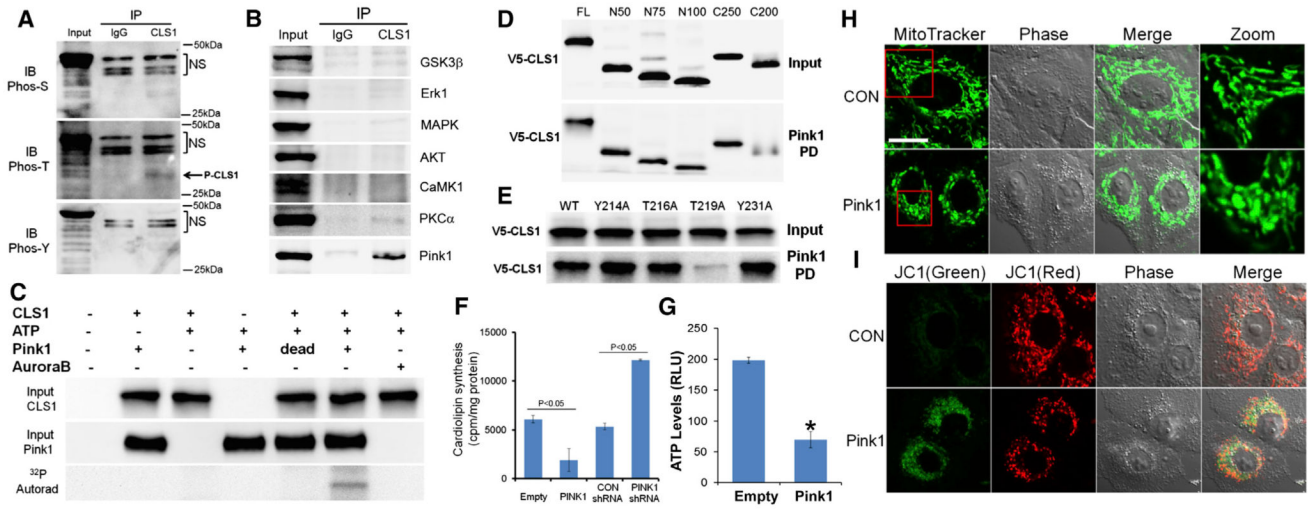

Figure 3. PINK1 Regulates CLS1 Protein Stability

(A) A549 cells were collected followed by coimmunoprecipitation of endogenous CLS1 and then probed with phospho antibodies in immunoblotting. IB, immunoblotting; IgG, immunoglobulin G; NS, nonspecific bands.

(B) Cells were collected followed by coimmunoprecipitation of endogenous CLS1 and then probed for kinases in immunoblotting.

(C) In vitro kinase assay. CLS1 protein was incubated with immunoprecipitated PINK1 and [^{32}P]γ-ATP under different assay conditions. Reaction mixtures were then resolved on SDS-PAGE before CLS1, PINK1 immunoblotting, and autoradiography.

(D and E) PINK1 was immunoprecipitated using PINK1 antibody and coupled to IgG beads. PINK1 beads were then incubated with in-vitro-synthesized products expressing his-V5-CLS1 mutants (top blots). After washing, proteins were eluted and processed for V5-CLS1 immunoblotting (bottom blots).

(F) Cells were transfected with empty plasmid, control shRNA, *PINK1*-shRNA, or a plasmid encoding *PINK1* for 48 hr. Cells were labeled with [^{3}H]-palmitic acid for an additional 24 hr. Cardiolipin synthesis was assayed and graphed (n = 3 experiments; *p < 0.05 versus CON or empty).

(G) ATP levels were assayed in transfected cells (n = 5 experiments; *p < 0.01 versus empty). Results in (F) and (G) are presented as mean ± SE.

(H and I) A549 cells were transfected with *PINK1* plasmid before being stained with MitoTracker Green (H) or JC-1 (I). Scale bar represents 10 μM.

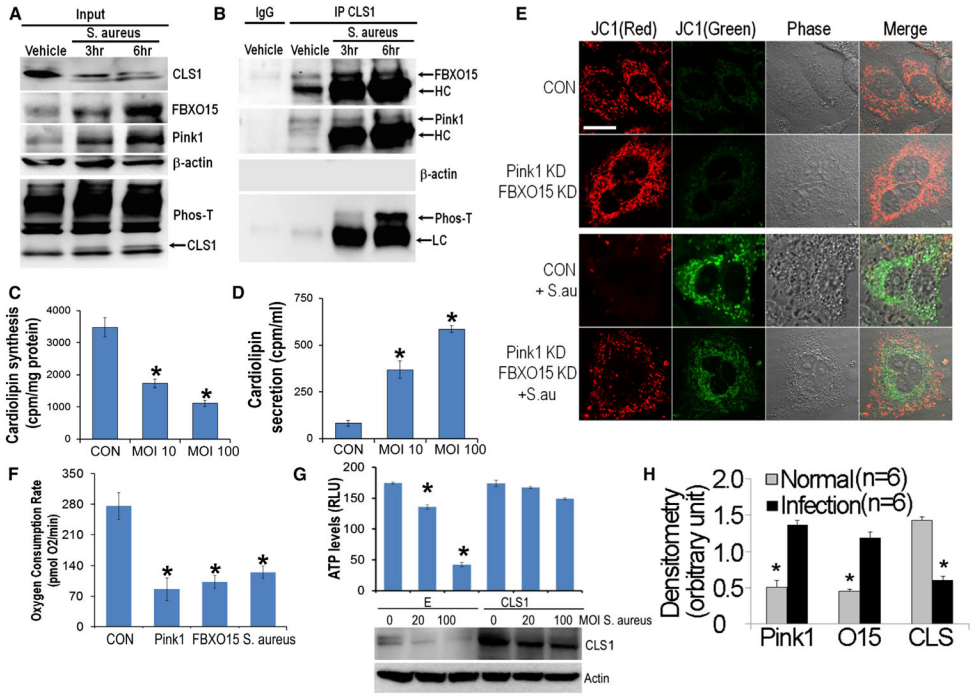

Figure 4. *S. aureus* Impairs Cardiolipin Biosynthesis and Mitochondrial Function

(A) *S. aureus* was given to mice (1×10^7 cfus/mouse i.t.) for 3 hr and 6 hr. Mice were euthanized and lungs harvested and assayed for CLS1, Fbxo15, PINK1, actin, and phospho-threonine (phospho-T) protein levels.

(B) Lung tissues from (A) were collected, lysed, and subjected to CLS1 IP, followed by Fbxo15, PINK1, actin, and phospho-threonine immunoblotting. HC, heavy chain; LC, light chain.

(C and D) A549 cells were infected with *S. aureus* at moi = 10 and 100 for 16 hr before labeling with [^{3}H]-palmitic acid and assayed for cardiolipin production (C) and secretion (D).

(E) Cells were transfected with CON shRNA, *PINK1*-shRNA, and/or *Fbxo15*-shRNA before exposure to *S. aureus* (*S. au*). Cells were then stained with JC-1 and observed under confocal microscopy.

(F) A549 cells were transfected with plasmids encoding either *Fbxo15* or *PINK1* or exposed to *S. aureus* at moi = 50 for 16 hr; cells were washed and analyzed using Seahorse technology to measure oxygen consumption rates.

(G) A549 cells were transfected with either empty plasmid or *CLS1* plasmid for 24 hr before exposure to *S. aureus* at moi = 20 or 100. Cells were then collected and assayed for ATP levels and CLS1 immunoblotting. n = 3 experiments; *p < 0.05 versus 0 moi.

(H) Human lungs (n = 6 control and six pneumonia lung tissue samples) were assayed for CLS1, Fbxo15, and PINK1 protein levels by immunoblotting; relative protein levels were graphed using densitometry (n = 3 in C, D, and G; n = 4 in F; n = 6 in H; *p < 0.05 versus CON in C, D, F, and H; data presented as mean ± SE).

Scale bar represents 10 μM.

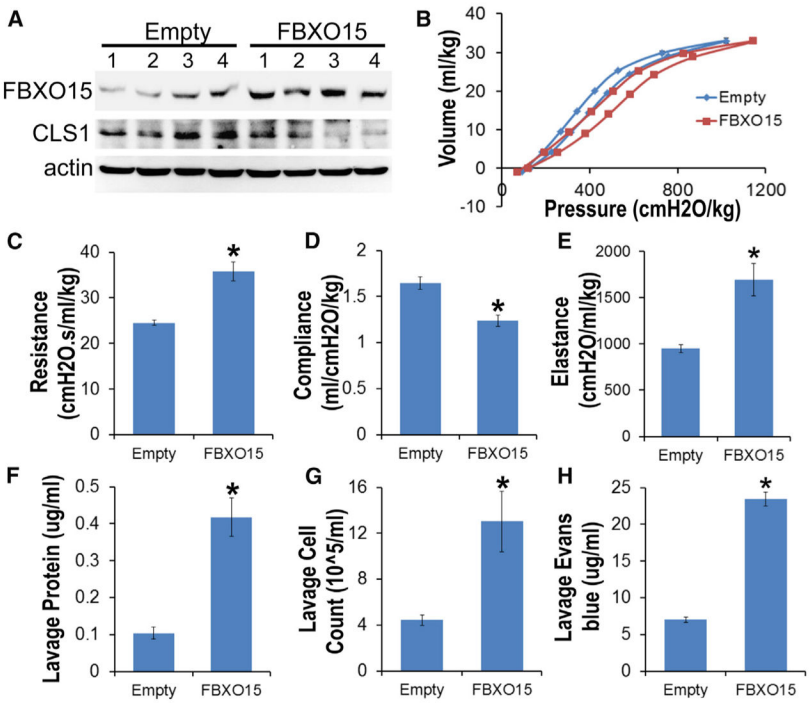

Figure 5. Fbxo15 Produces Acute Lung Injury

(A) C57BL6 mice (n = 4 mice/group) were given empty virus or a lentivirus encoding *Fbxo15* (10^8 plaque-forming units/mouse) for 96 hr. Mice were euthanized and lungs were assayed for Fbxo15 and CLS1 by immunoblotting.

(B–E) Before euthanization, animals were mechanically ventilated using Flexivent and lung compliance (B and D), resistance (C), and elastance (lung stiffness, E) were measured and graphed.

(F and G) Lavage protein and total cells counts. (H) Lung edema. Mice were assessed for Evans Blue dye extravasation in lung fluid. (*$p < 0.05$ versus empty in C–H; data presented as mean ± SE).

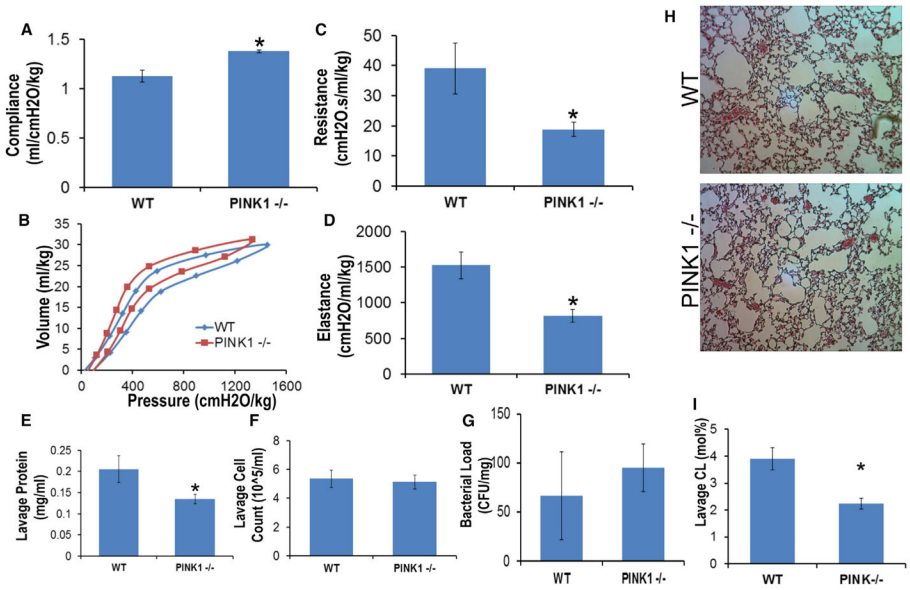

Figure 6. Pink1-Deficient Mice Have Less Pulmonary Injury after *S. aureus* Infection

Wild-type (WT) and PINK1 knockout mice (n = 6 mice/group) were infected with *S. aureus* (10^5 cfus/mouse i.t.) for 24 hr. Mice were then mechanically ventilated using Flexivent and lung compliance (A and B), resistance (C), and elastance (D) were measured and graphed. Lavage protein, cells counts, lavage bacterial loads, and lung histology are shown in (E)–(H). Cardiolipin (CL) levels are shown in (I) (*$p < 0.05$ versus WT in A–E, I; data presented as mean ± SE).

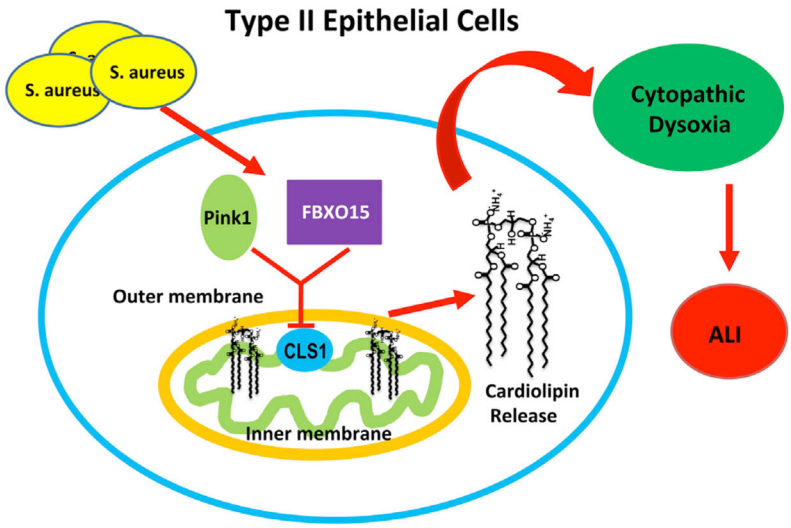

Figure 7. Model of Mitochondrial Damage during ALI

S. aureus infection induces expression of a kinase, PINK1, that phosphorylates an indispensable protein CLS1, which in turn triggers CLS1 ubiquitination and degradation by the F box protein (SCF^{Fbxo15}), leading to decreased cardiolipin production, extracellular release of a preformed pool of cardiolipin, and mitochondrial dysfunction. Fbxo15-PINK1 activation may contribute to cytopathic dysoxia observed in pneumonia. This pathway partakes in the pathobiology of pneumonia and acute lung injury (ALI).